Journal of Research in Medical and Dental Science
2024, Volume 12, Issue 5, Page No: 11-22

Available Online at: www.jrmds.in
eISSN No. 2347-2367: pISSN No. 2347-2545

Adsorption of Malachite Green from Aqueous Solution by Chitosan Assisted Silver Nanoparticles (Agnp): Isotherm Studies

A.A. Bamigbade*, K.D. Oduntan, J.T. Bamgbose

Department of Chemistry, College of Physical Sciences, Federal University of Agriculture, Nigeria

ABSTRACT

Malachite green dye adsorption from aqueous solution using silver nanoparticle (AgNP) stabilized with sodium tripolyphosphate cross-linked chitosan is reported in this study. Silver nanoparticle prepared was characterized by Fourier transform Infra-red spectroscopy (FTIR), X-ray diffractometry (XRD), UV-visible spectrophotometer and Scanning electron microscopy (SEM). The crystalline nature of the AgNP was revealed with XRD. The cubic face-centered structure of the synthesized silver nanoparticle was confirmed. This was supported by the observed sharp four diffraction peaks with peaks intense appeared at 2θ = 38.09°, 44.15°, 64.67°, and 77.54°. However, the SEM micrograph of the synthesized AgNP revealed the spherical shape of AgNP with a non-uniform granular shape attributed to bio-mediated ionic gelation process. The surface of the synthesized AgNP has a spherical shape and slightly elongated with a big tendency to aggregate and form larger particle clusters. Whereas, FTIR spectra of AgNP gave peaks at 1054 – 1645 cm-1 suggesting the presence of phosphonate linkages between ammonium, -NH3+ of chitosan and –PO32- moieties of NaTPP during cross linking process. The adsorption study was carried out under different conditions such as, pH, adsorbent dosage, contact time, temperature and initial concentration of dye to determine the best conditions and the maximum adsorption capacities. The results indicated that increase in temperature had very minimal effect on the adsorption process. The silver nanoparticle was effective in the removal of malachite green in acidic medium. This observation may be due to strong adsorption of the dye on the acidic surface of silver nanoparticle adsorbent by an acid-base interaction mechanism between the adsorbents and the adsorbates. Thus, the adsorption mechanism can be best described by electrostatic interaction. Langmuir, Freundlich and Tempkin model gave a better fit to adsorption isotherms while Dubinin Radushkevich model is not appropriate for the adsorption process. The results obtained from this study indicate that silver nanoparticle could be utilized as effective adsorbents for the removal of dyes from aqueous solution.

Key words: Silver nanoparticle; Sodium tripolyphosphate; Malachite green; Characterization; Adsorption

HOW TO CITE THIS ARTICLE: A.A. Bamigbade, K.D. Oduntan, J.T. Bamgbose. Adsorption of Malachite Green from Aqueous Solution by Chitosan Assisted Silver Nanoparticles (Agnp): Isotherm Studies. J Res Med Dent Sci, 2024; 12(5):11-22.

Corresponding author: A.A. Bamigbade
E-mail✉: akeemadesina1983@gmail.com
Received: 28-Apr-2024, Manuscript No. jrmds-24-137507;
Editor assigned: 01-May -2024, PreQC No. jrmds-24-137507 (PQ);
Reviewed: 15-May -2024, QC No. jrmds-24-137507 (Q);
Revised: 20-May-2024, Manuscript No. jrmds-24-137507 (R);
Published: 27-May-2024

INTRODUCTION

Nanoparticles are tiny particles that are between 1-100 nanometres in size [1]. They are so small that they are invisible to the naked eye, but they are potentially useful for human well-being in a wide range of applications in various fields such as medicine, electronics, optic, electronic, catalytic and materials science [2]. The unique properties of nanoparticles, such as their high surface area to volume ratio, controlled size, shape, and disparity make them attractive for use in a variety of applications [3]. Among all nanoparticles, noble metal nanoparticles have enormous applications in diverse areas such as bio-imaging, sensor, diagnosis, and novel therapeutic in biomedical field [4]. Metal materials in nanomaterial size or also known as metal nanomaterials are currently widely used as objects of research because they have several advantages compared to their bulk size, such as unique optical properties, physical properties and chemical reactivity [5]. Some applications of metal nanomaterials include colorimetric sensors for various analyte [6-7], conductors [8], anti-microbial and anti-bacterial [9-10],

energy conversion. One of the widely used metal nanomaterials is silver nanoparticles.

Silver nanoparticles have an interesting morphology, size, and different maximum thermal conductivity compared to other types of metal [11]. In addition, silver nanoparticles have good compound reactivity with relatively good abundance, essential physical properties and a lower price compared to other types of metals [12]. Therefore, silver nanoparticles are more widely used in various types of applications. Recently, silver nanoparticle was applied as antimicrobial agents in various products such as cosmetics [13], animal feed [14], Coating of catheters [15], wound dressing [16], and water purification [17] with a minimal risk of toxicity in humans. Some methods have been developed to synthesize silver nanoparticles such as chemical reduction [18], using Ketapang leaf extract [19], using Using Syzygium polyanthum Extract [20] and using Mangosteen bark extract [21]. Silver nanoparticles by chemical reduction can use a NaBH4 as a reducing agent. However, silver nanoparticles have a low stability and are able to easily aggregate forming flocks with larger size. Therefore, the other materials as a capping agent of silver nanoparticles are needed to prevent the aggregation between the surfaces of silver nanoparticles. Stabilization of silver nanoparticles with a polymer can improve the stability, electro-optical properties and biological applications. Polymers can bind to the surface of metal nanoparticles with several interactions such as a chemical adsorption, electrostatic interactions and hydrophobic interactions. Polymers that can be used as stabilizers for silver nanoparticles include Poly-(propyleneimine) Dendrimer (PPI), Poly- (vinylpyrrolidone) (PVP) and Hyperbranced Polyethylenimine (PEI). Chitosan was used in this study as a capping agent for silver nanoparticles. Chitosan (1-4-2-amino- 2-deoxy-D-glucosamine) is a linear polysaccharide which consists of N-acetylglucosamine and D- glucosamine. Chitosan has a –NH2 group that can interact with the surface of silver nanoparticles. Malachite Green (MG) (4-[(4-dimethylaminophenyl) phenylmethyl]-N,N-dimethylaniline) is an organic compound that has numerous industrial applications such as dyeing of silk, leather, plastics and paper. Their appearance is harmful to humans and animals following inhalation and/or ingestion, produces toxicity to respiratory system and reduces fertility in humans. It is highly toxic to mammalian cells, carcinogenic and can cause skin irritation. Therefore, removal of Malachite Green from effluent is essential to protect the environment. MG has high resistance to light and oxidizing agents, while its removal based on biological treatment and chemical precipitation has low efficiency. Conventional biological treatment in removing dyes from wastewaters is generally ineffective as the dyes are resistant to microorganisms. Moreover, the physico-chemical treatment methods are ineffective at higher effluent concentrations. It is now established that Ag is considered a promising semiconductor that is extensively involved in removal of several toxic organic containments through both adsorption and photo-catalytic process due to the stability of its chemical structure, biocompatibility, strong oxidizing power, non-toxicity and low cost of the metal precursors. In recent years, Nanotechnology has been extended to the wastewater treatments. Due to high surface area AgNPs exhibits an enhanced reactivity. In this study, we successfully reported the biosynthesis of silver nanoparticles using sodium tripolyphosphate cross-linked chitosan. Synthesized silver nanoparticles were used to remove dye from aqueous solution via adsorption process.

MATERIALS AND METHODS

Chitosan produced from lobster shell wastes with 85% degree of deacetylation, Hydrochloric acid, glacial acetic acid, Sodium hydroxide were supplied by Aldrich. Sodium borohydride, sodium Tripolyphosphate (TTP), Silver nitrate, acetone and Ethanol were obtained from Sigma Chemical and Co and used as received. Malachite green was obtained from Bektoh (Germany) and used without further purification. It was characterized by its visible spectrum, which gave a molar extinction coefficient which is in agreement with the literature value at λmax of 619 nm. All solutions were prepared with double distilled water, and all chemicals were used without further purification.Characterization of silver nanoparticle was done, using both atomic and scanning devices which included: XRD–X-ray Diffraction crystallography, Fourier Transform Infra-Red Spectrophotometer (FTIR),

SEM - Scanning Electron Microscopy and UV-Visible Spectroscopy

Preparation and characterization of silver-chitosan Nanoparticle (AgNP)

A silver-chitosan nanoparticle (AgNP) was prepared according to a modified literature procedures .60mgof chitosan was dissolved in 20 mL of 2% acetic acid to obtain chitosan solution. 0.25% of TPP solution was added to chitosan solution in the ratio of 1:3 TTP to chitosan, with mild stirring until an opalescent suspension is obtained. 10 mL of 0.37% of silver nitrate solution was added to the chitosan-TTP hydrogel and stirred continuously for 30 minutes to obtain homogeneous solution. Final stage of the synthesis was the addition of 10 mL of 0.01M sodium borohydride. AgNO3/Chitosan-TTP gelatin is a colourless solution, but once the reducing agent NaBH4 was introduce to the polymers suspensions, there was immediate colour change to dark brown, indicating the formation of silver nanoparticle. The chitosan-silver nanoparticle was separated from the liquid by centrifugation for one hour at 10,000 g. The supernatant was discarded and the particles were washed thoroughly with acetone, ethanol, distilled water and then vacuum filtered. The obtained particles were oven-dried at 110ºC.

The silver nanoparticle prepared was characterized using Fourier-Transformed Infra-Red Spectroscopy (FTIR), X-ray Diffractometer (XRD), Transmission Electron Microscopy (TEM), and Scanning Electron Microscope (SEM).

Schematic representation of reaction path for the preparation of the Chitosan-silver nanoparticle

Adsorption studies

Adsorption studies were carried out following a procedure. Stock solution (100 mg/L) of Malachite green dye was prepared by dissolving 0.1 g of the dye in 1000 ml of water; 50 mg/L of the dye were prepared from the stock solution. Silver nanoparticle adsorbent (0.02 g) was then added to the prepared solutions separately and the mixtures were shaken for 2 h. Absorbance readings were taken using the UV-Visible spectrophotometer (Shimada UV spectrophotometer, UV- 1800) at a λmax of 420 nm. The effect of concentration, temperature, time, pH, and adsorbent dosage on the adsorption process was also determined and absorbance before and after the adsorption process was taken to determine the quantity (qe) of Malachite green (mg/g) dye adsorbed at equilibrium using the formula:

$$q_e = \left(\frac{C_o - C_e}{m}\right) \times v$$

Where Co and Ce (mg/L) are the initial and final concentrations of the adsorbates respectively, v is the volume of the solution used (ml) and m is the mass (g) of the adsorbents. The effect of time was studied at time interval of 10–90 minutes, while the effect of temperature was studied at

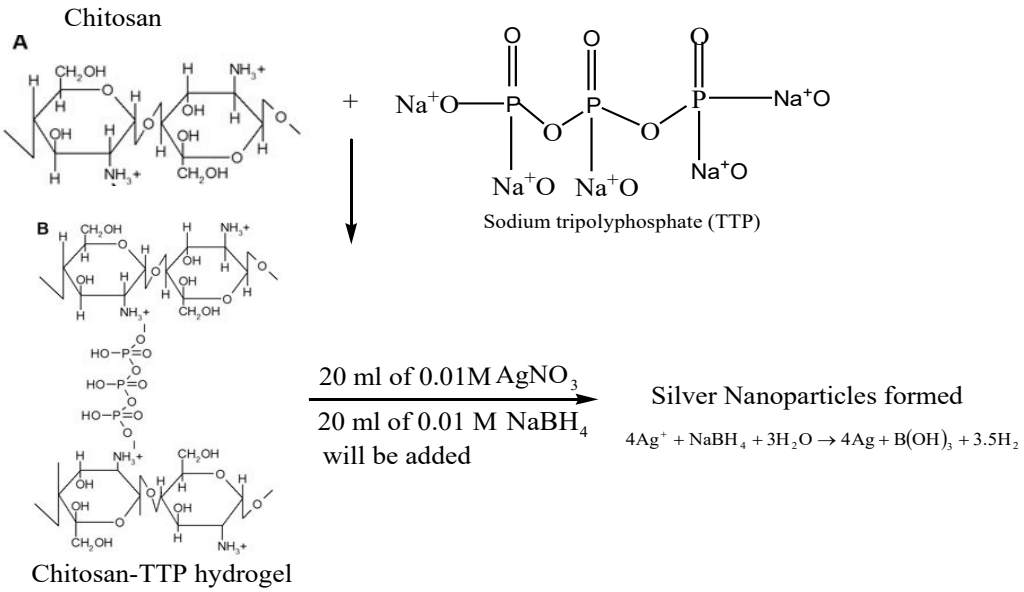

Note: The positive charges on the amino groups of chitosan resulting from its dissolution in acetic acid interact with the negative charges on the tripolyphosphate anions, causing ionic-gelation and formation of hydrogel.

temperature range of 10–40 oC. The effect of pH was studied by varying the pH between 2–13 using 0.1 M HCl or 0.1 M NaOH, while the effect of concentration was studied using 50–250 mg/L of the adsorbate.

Characterizations of Silver Nanoparticle (AgNP)

The brown colour silver nanoparticle solution which arises due to excitation of surface Plasmon vibrations of the silver nanoparticles was subjected to UV-Visi¬ble spectra recording using Shimadzu UV-1601double beam spec¬trometer with quartz cuvettes of 1cm path length. The UV-Visible spectrum of AgNP was presented in (Figure 1). The Surface Plasmon Resonance (SPR) peak of AgNP which is equivalent to maximum absorbance peak found to occur at 420nm. AgNPs with size range 7-10 nm most¬ly show the SPR peaks at 420nm. The overall observations suggest that the bio reduction of (silver ions) Ag+ to Ag0 was confirmed by UV-Visible spectroscopy. FTIR spectra are recorded in KBr pellets for the pure capping agent chitosan cross-linked with sodium triployphosphate stabilized AgNP at 25oC using ABBBOMEM MB 3000 Instrument. SEM photograph of the chitosan stabilized AgNP are measured using Hitachi SU 6600 Instrument. The phase variety and grain size of synthesized silver nanoparticles was determined by X-ray diffraction spectroscopy (Philips PAN analytical). The synthesized nanoparticle was studies with Cu-Kα radiation at voltage of 30 kV and current of 20 mA with scan rate of 0.03 o/s, λ = 1.54 Å. The morphological features of synthesized silver nanoparticles were studied by NOVA Nano - Scanning Electron Microscope (JSM - 6480 LV). The SEM slides were prepared by making a smear of the solutions on slides. A thin layer of platinum was coated to make the samples conductive. Then the samples were characterized in the SEM at an accelerating voltage of 5 KV, emission current of 75 – 80 A and working distance of 6–13 nm.

RESULTS AND DISCUSSION

Results of X-ray Diffraction Spectroscopy

The XRD diffraction pattern presented in (Figure 1) shows that silver nanoparticles have been synthesized. The structures of the silver nanoparticles produced confirm the cubic face-centered structure of silver nanoparticle. This was validated by the observed sharp four diffraction peaks with peaks intense appeared at 2θ = 38.09°, 44.15°, 64.67°, and 77.54° as shown in (Figure 1) which are indexed to 111, 200, 220, and 311 Bragg's reflection, respectively show the crystalline structure of silver nanoparticles. The obtained data was matched with JCPDS card no. (65-2871) and the sharpness of the peak clearly shows that the particles are crystalline in nature. The crystallite size of the obtained silver nanoparticles were calculated to be 16 nm using Debye-Scherrer Equation ($D = k\lambda/\beta\cos\theta$) with a relative deviation of 4.65%, where D is the average crystallite size of the nanoparticles, k is the is geometric factor called Scherrer constant with a value of 0.9, λ is the wavelength of X-ray

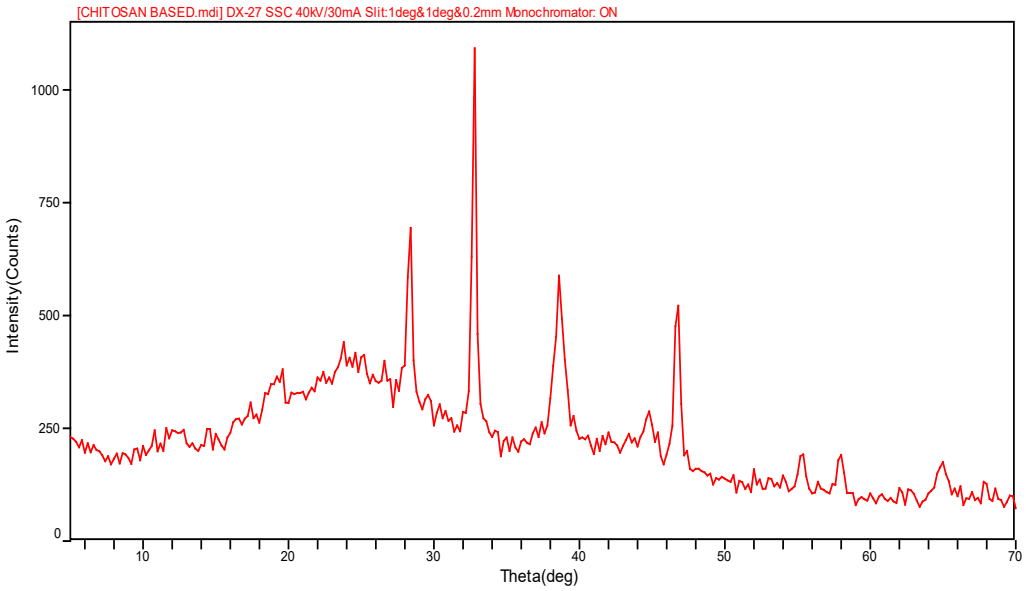

Figure 1: XRD spectrum of Silver Nanoparticle (AgNP).

radiation source (0.15406 nm), θ is the Bragg's angle and β is the angular full-width at half maximum (FWHM = 0.004) of the XRD peak at the diffraction angle θ. XRD patterns (JCPDS, File No. 04–0783) and the structure of prepared silver nanoparticles were found to be face-centered cubic (FCC) crystal.

Results of SEM analysis of silver nanoparticle

SEM analysis was carried out to determine particle morphology. Image enlargement of silver nanoparticles was carried out on a scale of 80 μm with HV 5.0 Kv as presented in (Figure 2). The surface morphology of silver nanoparticles is relatively smooth, smooth, spherical shape, high density structure with a non-uniform granular shape attributed to bio-mediated ionic gelation process. The morphology of the synthesized silver nanoparticles has a spherical shape and slightly elongated with a big tendency to aggregate and form larger particle clusters this observation is similar to what was reported by.

Results of UV-visible for Silver Nanoparticle

The brown colored silver nanoparticle solution which arises due to excitation of surface Plasmon vibrations of the silver nanoparticles was subjected to UV-Visi¬ble spectra recording using Shimadzu UV-1601 double beam spec¬trometer with quartz cuvettes of 1cm path length. The UV-Visible spectrum of AgNP was presented in (Figure 3). The Surface Plasmon Resonance (SPR) peak of AgNP which is equivalent to maximum absorbance peak occurred at 420nm. It has been reported that AgNPs with size range 7-10 nm most¬ly show the SPR peaks at 420nm.

The absorbance and broadening of the peak at around 420 nm indicates that the particles were mono-dispersed and indicating the Surface Plasmon Resonance (SPR) absorption band due to the combined vibration of electrons in resonance with UV-visible light . The overall observations suggest that the bio reduction of (silver ions) Ag+ to Ag0 was confirmed by UV-Visible spectroscopy (Figure 3).

Results of FTIR Silver Nanoparticle

The IR spectra of silver nanoparticle shown in (Figure 4) gave peaks at 1054 – 1308 cm-1 suggesting the presence of phosphonate linkages between ammonium, -NH3+ of chitosan and –PO32- moieties of NaTPP during cross linking process. The spectrum showed two peaks, one at 1140 cm-1 and another at 1279 cm-1, indicating symmetric and asymmetric stretching of phosphonate linkage, respectively, the asymmetric peak is known to occur due to restricted rotation. The two terminals –PO32- groups of NaTPP molecule appears to be connected with two -NH3+, (CH3COO-) groups of two chitosan monomers. The nanoparticle exhibit a broadening of the band beginning at approximately 3500 cm–1 and extending to and almost obscuring the CH2 stretching region around 2900 cm–1. There is also and a loss of the small features on the band. This broadening is indicative of increased intermolecular hydrogen bonding between NH and OH. A maximum

Figure 2: Scanning Electron Micrograph (SEM) of AgNP.

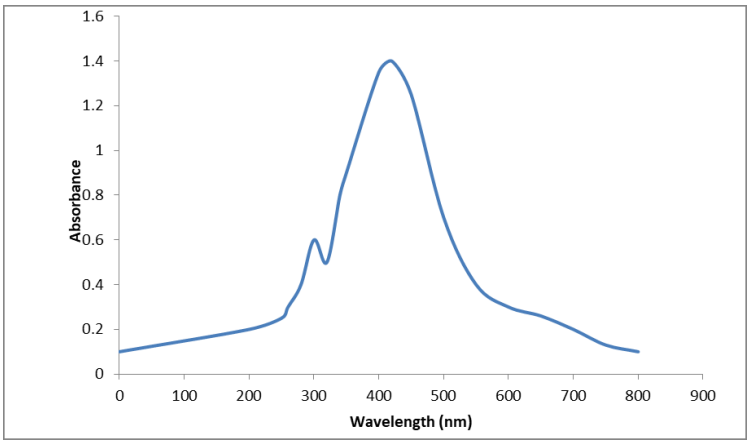

Figure 3: UV-visible spectrum of Silver Nanoparticle (AgNP).

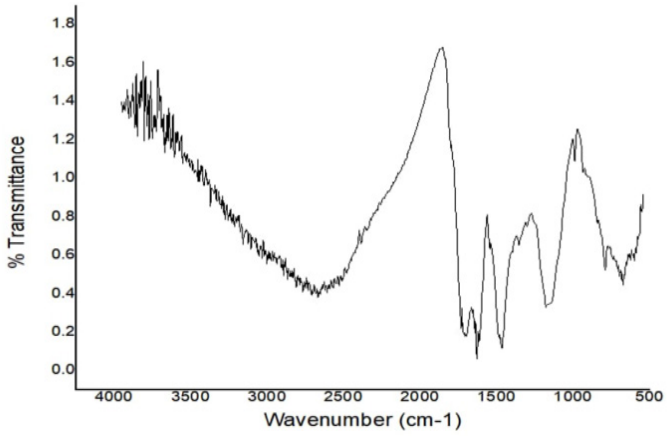

Figure 4: FTIR spectrum of Silver Nanoparticle (AgNP).

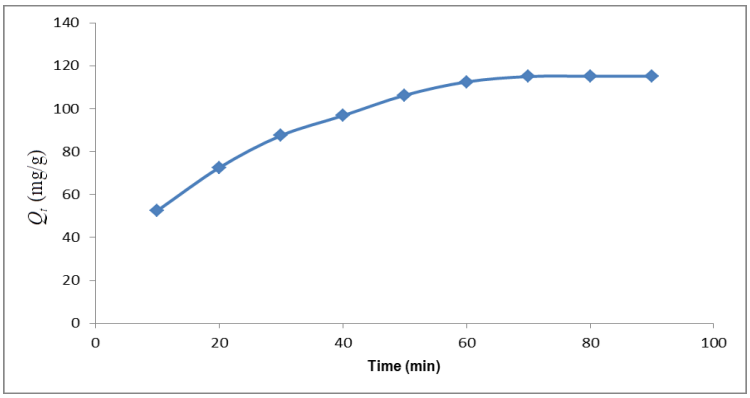

Figure 5: Percentage Dye removed with time.

at approximately 3180 cm–1 is exhibited by the silver nanoparticle. This band broadening is similar to that found in the literature for chitosan-TTP nanoparticles and for chitosan succinlyated nanoparticles and is attributed to the formation of hydrogen bonded networks. The AgNP show a low intensity but very broad band centred around 3263 cm–1. This suggests that silver chitosan complexes prepared contain mostly nanoparticles.

Adsorption studies

Effect of contact time

The effect of contact time on the adsorption of Malachite green onto the adsorbents was studied at pH 8.0 using 50 mg/L of dye, and 0.02 g adsorbent dosage for 10–90 min in order to determine the equilibrium time for the adsorption processes. The result of the study shown in (Figure 5) indicates that the adsorption efficiency increased gradually with increase in

contact time and reached a maximum value after 60 min for silver nanoparticle. The adsorption of the dye on the adsorbents remained constant afterwards. The increase in adsorption at the beginning of the process is due largely to the availability of adsorption sites, which became occupied with time in the course of the adsorption process making further adsorption onto the adsorbents to be insignificant.

Effect of pH

As shown in (Figure 6) the effect of pH on the adsorption of Malachite green onto the adsorbents. The effect was studied using the equilibrium concentrations for the adsorbents (i.e. 25 mg/L) for a period of 60 min for the experiment, while the pH was varied from 2.0 – 13.0 using 0.1 M HCl or 0.1 M NaOH. It can be seen from (Figure 6) that adsorption of the malachite green onto silver nanoparticle increased with pH values, reaching the optimum sorption process at around pH 4.7. This observation may be due to the increased degradation of malachite green dye. The negative charges at the surface of AgNP were being neutralization via an acid-base interaction mechanism between the adsorbents and the adsorbates, which subsequently enhances the diffusion phenomena to occur, and additional active sites are available for the adsorption process. Thus, the adsorption mechanism can be best described by electrostatic interaction. However, at the pH below 4, the dye degradation and the number of negatively charged adsorbent sites decrease. The increasing in the number of positively charged active surface sites enhances the dye-adsorbent repulsion, which decreases the efficiency of the adsorption process. At a lower pH, the malachite green adsorption improved due to the acidic media. As pH increases, the adsorbent surface becomes more negatively charges, and these are responsible for increasing the adsorption capacity due to the electrostatic interaction. However, the adsorption of malachite green dye was observed decreasing at high pH. But at pH 7 the sorption process was observed to be decreasing with increasing pH values. This observation may be as results of the interaction between the carboxylic groups of the chitosan present in the caped material for the nanoparticle and water predominates over the interaction between the adsorbent and the dye, hence the reduced adsorption. The synergic influences of both phenomena significantly suggest strong influence of the solution pH on Malachite green adsorption.

Effect of temperature

The effect of temperature on the adsorption of Malachite green dye onto the adsorbents was studied using the equilibrium solution concentration for each of the adsorbents while the temperature was varied from 10–40 oC, for a period of 60 min for each experiment. The result of the study shown in the (Figure 7) indicated that increase in temperature had very minimal effect on the adsorption process.

Equilibrium adsorption isotherm studies

Equilibrium adsorption isotherms are required to give useful information about mechanism, properties, and tendency of adsorbent to adsorb the Malachite green. Various isotherms models (Langmuir, Freundlich, Tempkin, and Dubinin–Radushkevich [D–R]) were used to discuss the equilibrium characteristics of the process of adsorption. The plotted graphs are shown in

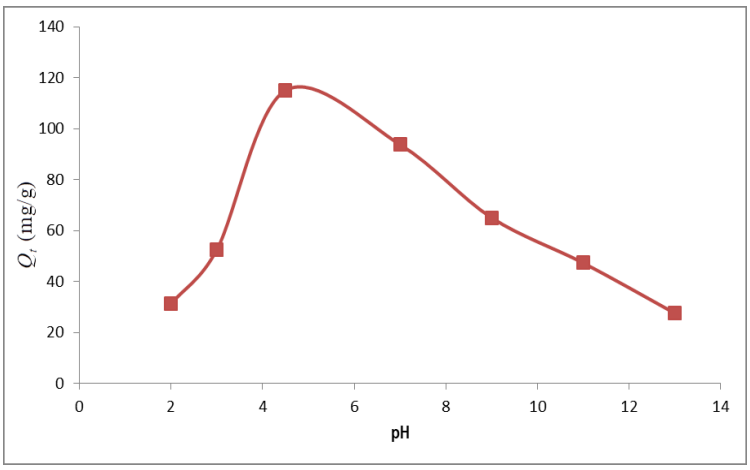

Figure 6: Percentage Dye removed with pH.

(Figure 8) and the constant parameters of the isotherm equations for this adsorption process are summarized in (Table 1).

Arising from the linear form of Langmuir isotherm model, the values of [the Langmuir adsorption constant (L/mg)] and [theoretical maximum adsorption capacity (mg/g)] were obtained from the intercept and slope of the plot of versus, respectively. The Langmuir isotherm assumes a monolayer adsorption onto a solid surface with a definite number of identical sites and there is no interaction between the adsorbate molecules. The fitness of experimental data was evaluated for 0.02 g each of the adsorbents. The high correlation coefficient of 0.9834 for the silver nanoparticle adsorbents over the optimized concentration strongly supports the fact that the adsorption data closely follow the Langmuir model. The Langmuir monolayer capacity being 58.24 mg of Malachite green per gram of silver nanoparticle adsorbent suggests that it exhibits the highest relevant adsorption properties. To confirm this result, the favorable or unfavorable Malachite green adsorption by Langmuir model was determined from calculation of the separation factor (RL) as follows: where (L/mg) is the Langmuir constant and (mg/L) is the initial concentration. The adsorption process can be determined as favorable when the RL value lies between 0 and 1. It was found that silver nanoparticle adsorbents the RL values

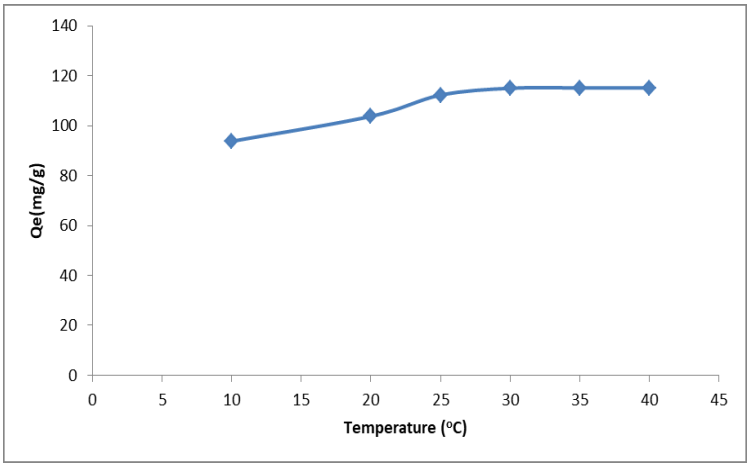

Figure 7: Percentage Dye removed with temperature.

Table 1. The coefficients isotherm parameters for Malachite green adsorption onto Silver nanoparticle.

ISOTHERMS	EQUATIONS	CONSTANTS	ADSORBENTS Silver Nanoparticle
LANGMUIR	$\frac{C_e}{q_e} = \frac{1}{K_a Q_e} + \frac{C_e}{Q_e}$	Q_e (mg/g)	58.80
		K_a (L mg^{-1})	0.54
		R_L	0.07
		R^2	0.9834
FREUNDLICH	$\ln q_e = \ln K_f + \left(\frac{1}{n}\right)\ln C_e$	$\frac{1}{n}$	6.38
		n	2.02
		$\frac{1}{n}$	0.49
		R^2	0.9746
		B_1 **(mg/g)**	12.65
TEMPKIN	$q_e = B_1 \ln K_T + B_1 \ln C_e$	K_T	8.01
		R^2	0.9889
DUBININ-RADUSHKEVIC	$\ln q_e = \ln Q_s - B\varepsilon^2$	Q_S	210.12
		E (kJ/mol)	808.25
		B	-222.27
		R^2	0.3817

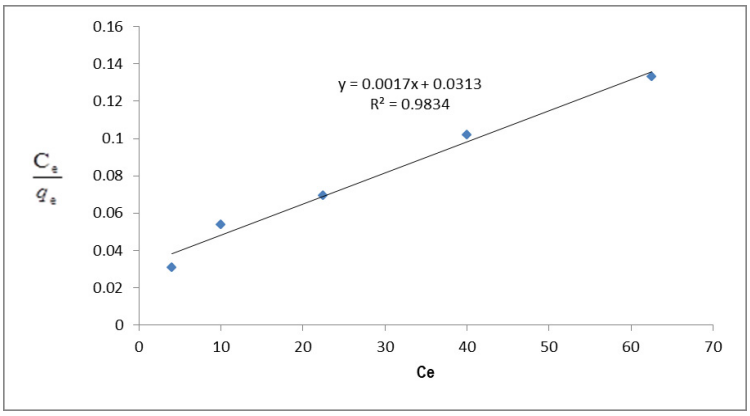

Figure 8: Plot of $\frac{C_e}{q_e}$ versus.

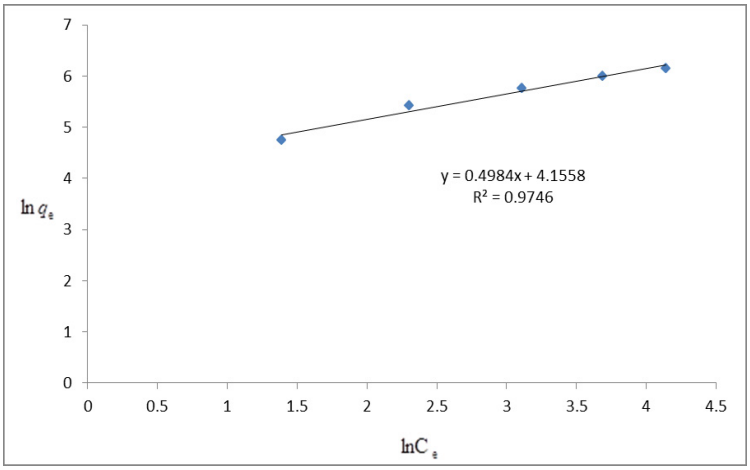

Figure 9: Plot of $\ln q_e$ versus $\ln C_e$.

are lower than 1, suggesting the favorable adsorption and the fitness of Langmuir model to the experimental data. The parameters of Freundlich isotherm model such as [(mg g−1)/ (mg L−1)] and were obtained from the intercept and slope of the linear plot of ln qe versus ln Ce, presented in (Figure 9).

K_f Is the Freundlich constant indicates the extent of adsorption, and $\frac{1}{n}$ is the heterogeneity factor (adsorption effectiveness). The $\frac{1}{n}$ value ranges between 0 and 1. When the value of $\frac{1}{n}$ is equal to unity, the adsorption is linear; when the value of $\frac{1}{n}$ is below the unity, the adsorption process is chemically driven; and when the value of $\frac{1}{n}$ is above the unity, adsorption is a physically driven process. The values of $\frac{1}{n}$ obtained is 0.49 indicating the favorability of adsorption and high tendency of Malachite green for the adsorption onto silver nanoparticle, while higher R^2 values of 0.9746 over the whole adsorbent dosage showed that the Freundlich model fit into the experimental data. The heat of the adsorption and the adsorbent–adsorbate interaction were calculated using Tempkin isotherm model. In this model, B_1 is the Tempkin constant related to heat of the adsorption (J/mol), T is the absolute temperature (K), R is the universal gas constant (8.314 J/mol/K) and K_T is the equilibrium binding constant (L/mg). The values of the Tempkin constants (8.01) and the correlation coefficient (0.9889) are analogous to the Freundlich and Langmuir values. Therefore, the Tempkin isotherm is fit into experimental data like both Langmuir and Freundlich isotherms (Figure 10).

D–R model was applied to estimate the porosity apparent free energy and the characteristic of adsorption. In this model, $K_{(\text{mol2/kJ2})}$ is a constant

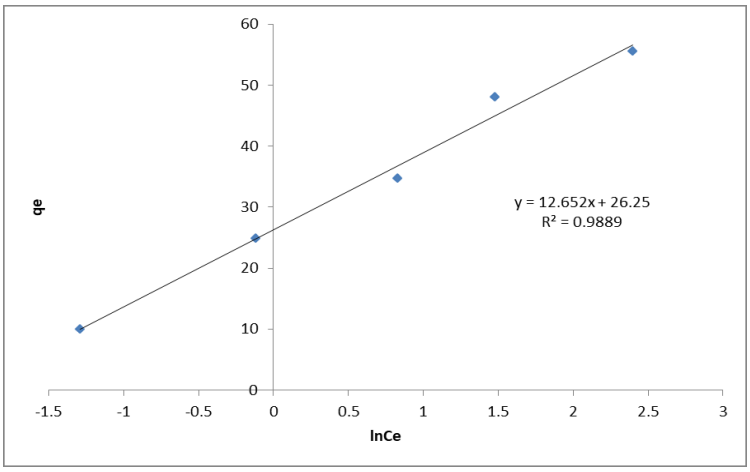

Figure 10: Plot of qe versus lnCe.

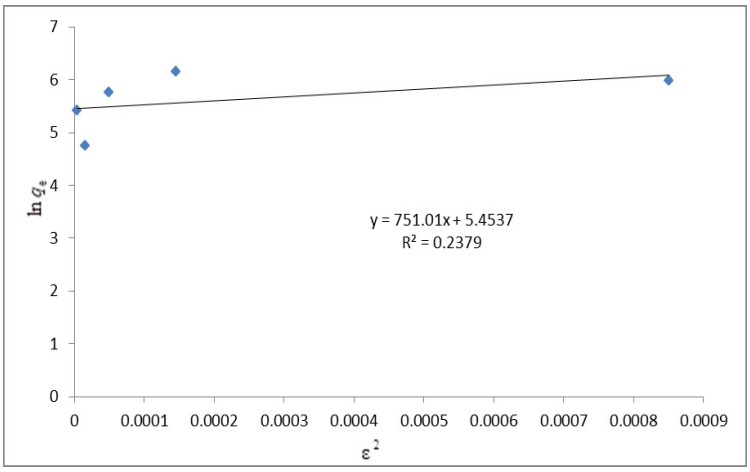

Figure 11: Plot of Inq_e versus $\mathcal{E}^2$.

related to the adsorption energy, Qs (mg/g) is the theoretical saturation capacity, and e is the Polanyi potential. The slope of the plot of Inq_e versus ε^2 in (Figure 11) gives B and the intercept yields the Qs value.

In this case, the D–R equation represents poor fit of the experimental data for silver nanoparticle. The fitting results showed that the correlation coefficient of Langmuir isotherm was higher than that of the other isotherms, indicating that the adsorption of malachite green on the adsorbent can better be described using Langmuir, Freundlich and Tempkin model and the adsorption is a monolayer adsorption while Dubinin Radushkevich model is not appropriate for the adsorption process .

CONCLUSION

Silver nanoparticle was prepared via ionic gelation process and characterized by Fourier transform Infra-Red Spectroscopy (FTIR), X-ray Diffractometry (XRD), UV-visible Spectrophotometer (UV-vis) and Scanning electron microscopy (SEM) in this study. The crystalline size of the AgNP was revealed with XRD. The cubic face-centered structure of the synthesized silver nanoparticle was confirmed. This was supported by the observed sharp four diffraction peaks with peaks intense appeared at 2θ = 38.09°, 44.15°, 64.67°, and 77.54°. However, the SEM micrograph of the synthesized AgNP revealed the spherical shape of AgNP with a non-uniform granular shape attributed to bio-mediated ionic gelation process. The surface of the synthesized AgNP has a spherical shape and slightly elongated with a big tendency to aggregate and form larger particle clusters. Whereas, FTIR spectra of AgNP gave peaks at 1054 – 1645 cm-1 suggesting the presence of phosphonate linkages between ammonium, -NH3+ of chitosan and –PO32- moieties of NaTPP during cross linking process. The silver nanoparticles synthesized were used

as adsorbents for the removal of malachite green from aqueous solution. The results showed that the prepared silver nanoparticle show high adsorption capacity for malachite green. The process of adsorption was fast and attained equilibrium within 60 min. The silver nanoparticle was found to be the most effective in the removal of malachite green due to the acid-base interaction between the adsorbent and the adsorbate as the malachite green solution is in the acidic medium. The effective pH for the study was found to be around 4.6 for the nanoparticle adsorbents, while the optimum adsorbent dose was 0.02 g. Langmuir, Freundlich and Tempkin model gave a better fit to adsorption isotherms while Dubinin Radushkevich model is not appropriate for the adsorption process. The kinetic study of malachite green onto silver nanoparticle adsorbents showed that the adsorption kinetics followed both the pseudo-first-order and pseudo-second-order rate. The results obtained from this study indicate that silver nanoparticle obtained using simple method like the one adopted in this research could be utilized as effective adsorbents for the removal of dyes from wastewater.

ACKNOWLEDGEMENT

The authors wish to thank the staff of Chemistry Department of Covenant University, Ota for their assistance in running the scanning electron micrograph of the nanoparticles. All others characterization of the nanoparticle were carried out at the chemistry Department, FUNAAB. The work was carried out in the postgraduate research laboratories of the Department of Chemistry, FUNAAB. We are grateful to the Management of Federal University of Agriculture, Abeokuta (FUNAAB) for the support in providing the equipment used in this research.

REFERENCES

1. Wang J, Koo Y, Alexander A, et al. Phytostimulation of poplars and Arabidopsis exposed to silver nanoparticles and Ag+ at sublethal concentrations. Environ Sci Technol. 2013; 47:5442-9.
2. Annamalai J, Nallamuthu T. Green synthesis of silver nanoparticles: characterization and determination of antibacterial potency. Appl Nanosci. 2016; 6:259-65.
3. Jia F, Liu X, Li L, et al. Multifunctional nanoparticles for targeted delivery of immune activating and cancer therapeutic agents. J Control Release. 2013; 172:1020-34.
4. Magalhães AP, Santos LB, Lopes LG, et al. Nanosilver application in dental cements. Int Sch Res Notices. 2012; 2012:365438.
5. Gangadharan D, Harshvardan K, Gnanasekar G, et al. Polymeric microspheres containing silver nanoparticles as a bactericidal agent for water disinfection. Water Res. 2010; 44:5481-7.
6. Barani H, Mahltig B. Microwave-assisted synthesis of silver nanoparticles: Effect of reaction temperature and precursor concentration on fluorescent property. J Clust Sci. 2022:1-1.
7. V. Shrivastava I, Ali MM, Marjub, et al. Nanocomposites via in-situ co-reduction of the oxides. Powder Technol. 2022;233, 208-214.
8. Choi O, Deng KK, Kim NJ, et al. The inhibitory effects of silver nanoparticles, silver ions, and silver chloride colloids on microbial growth. Water Res. 2008; 42:3066-74.
9. Ahmed T, Noman M, Shahid M,et al. Green synthesis of silver nanoparticles transformed synthetic textile dye into less toxic intermediate molecules through LC-MS analysis and treated the actual wastewater. Environ Res J. 2020; 191:110142.
10. Li Y, Sun S, Gao P, et al. A tough chitosan-alginate porous hydrogel prepared by simple foaming method. J Solid State Chem. 2021; 294:121797.
11. G. Prakash Z, Ahmad MZ, Manzoor, et al Optimization for biogenic microbial syn-thesis of silver nanoparticles through response surface. Langmuir. 2014; 27:720-726
12. Asmat U, Abad K, Ismail K. Diabetes mellitus and oxidative stress—A concise review. Saudi Pharm J. 2016; 24:547-53.
13. Khodadadi B, Bordbar M, Yeganeh-Faal A, et al. Green synthesis of Ag nanoparticles/clinoptilolite using Vaccinium macrocarpon fruit extract and its excellent catalytic activity for reduction of organic dyes. J Alloys Compd. 2017; 719:82-8.
14. Huang J, Li Q, Sun D, et al. Biosynthesis of silver and gold nanoparticles by novel sundried Cinnamomum camphora leaf. J Nanotechnol. 2007; 18:105104.
15. Kasthuri J, Kathiravan K, Rajendiran NJ. Phyllanthin-assisted biosynthesis of silver and gold nanoparticles: a novel biological approach. J Nanoparticle Res. 2009; 11:1075-85.
16. Chu DT, Sai DC, Luu QM, et al. Synthesis of bifunctional Fe 3 O 4 SiO 2-Ag magnetic–plasmonic nanoparticles by an ultrasound assisted chemical method. J Electron Mater. 2017 Jun; 46:3646-53.
17. Crini G, Badot PM. Application of chitosan, a natural aminopolysaccharide, for dye removal from aqueous solutions by adsorption processes using batch studies: A review of recent literature. Prog Polym Sci. 2008; 33:399-447.
18. Song J, Han G, Wang Y, et al. Pathway and kinetics of malachite green biodegradation by Pseudomonas veronii. Sci Rep. 2020; 10:4502.

19. W.Q. Ruan, X.D. Pan, F. Shen, et al. A review of recent advances in the catalytic synthesis of polyesters and biopolyesters. Chem Soc Rev. 2017; 46(16), 4819-4839.

20. Huang J, Li Q, Sun D, et al. Biosynthesis of silver and gold nanoparticles by novel sundried Cinnamomum camphora leaf. J Nanotechnol. 2007; 18:105104.

21. Zahoor M, Nazir N, Iftikhar M, et al. A review on silver nanoparticles: Classification, various methods of synthesis, and their potential roles in biomedical applications and water treatment. Water. 2021; 13:2216.